

# Incommensurate Magnetic Order and Dynamics Induced by Spinless Impurities in $\text{YBa}_2\text{Cu}_3\text{O}_{6.6}$

A. Suchaneck,<sup>1</sup> V. Hinkov,<sup>1</sup> D. Haug,<sup>1</sup> L. Schulz,<sup>2</sup> C. Bernhard,<sup>2</sup> A. Ivanov,<sup>3</sup> K. Hradil,<sup>4</sup> C. T. Lin,<sup>1</sup> P. Bourges,<sup>5</sup> B. Keimer,<sup>1,\*</sup> and Y. Sidis<sup>5,†</sup>

<sup>1</sup>Max Planck Institute for Solid State Research, D-70569 Stuttgart, Germany

<sup>2</sup>Physics Department and Fribourg Center for Nanomaterials, Fribourg University, CH-1700 Fribourg, Switzerland

<sup>3</sup>Institut Laue-Langevin, 156X, F-38042 Grenoble Cedex 9, France

<sup>4</sup>Institute for Physical Chemistry, University of Göttingen, D-37077 Göttingen, Germany

<sup>5</sup>Laboratoire Léon Brillouin, CEA-CNRS, CE-Saclay, F-91191 Gif-sur-Yvette, France

We report an inelastic-neutron-scattering and muon-spin-relaxation study of the effect of 2% spinless (Zn) impurities on the magnetic order and dynamics of  $\text{YBa}_2\text{Cu}_3\text{O}_{6.6}$ , an underdoped high-temperature superconductor that exhibits a prominent spin pseudogap in its normal state. Zn substitution induces static magnetic order at low temperatures and triggers a large-scale spectral-weight redistribution from the magnetic resonant mode at 38 meV into uniaxial, incommensurate spin excitations with energies well below the spin pseudogap. These observations indicate a competition between incommensurate magnetic order and superconductivity close to a quantum critical point. Comparison to prior data on  $\text{La}_{2-x}\text{Sr}_x\text{CuO}_4$  suggests that this behavior is universal for the layered copper oxides and analogous to impurity-induced magnetic order in one-dimensional quantum magnets.

PACS numbers: 75.10.Kt, 74.25.Dw, 74.72.Gh, 74.72.Kf

Spinless impurities have provided key insights into the spin correlations of low-dimensional quantum magnets. Research on quasi-one-dimensional (1D) quantum-disordered magnets with a spin gap has shown that every magnetic vacancy contributes to a Curie term in the uniform susceptibility and generates a cloud of antiferromagnetically correlated spins whose spatial extent is inversely proportional to the gap [1]. The striking discovery that a dilute concentration of spinless impurities induces antiferromagnetic long-range order in a spin-Peierls system [2] can be attributed to constructive interference between spin-polarization clouds centered at different impurities. Related “order-from-disorder” phenomena were later observed in a wide class of quasi-1D systems and shown to exhibit universal characteristics [3,4]. In contrast to the comprehensive understanding that has been developed for 1D magnets, theoretical work on spinless impurities in 2D quantum magnets has thus far been restricted to analytical calculations at quantum critical points [5–7] and numerical simulations for specific 2D spin Hamiltonians with quantum-disordered ground states [8]. Both approaches predict impurity-induced spin textures and order-from-disorder phenomena not unlike those observed in 1D magnets. Experimental tests of these predictions have, however, proven difficult because of the paucity of physical realizations of 2D spin liquids and the limited chemical solubility of nonmagnetic atoms in specific compounds.

Layered copper oxides have been a fruitful testing ground for theories of 2D quantum magnetism and for the behavior of spinless impurities in two dimensions, despite additional complications introduced by the presence of itinerant charge carriers and *d*-wave superconductivity [1,9]. Spinless impurities can be readily introduced

into the  $\text{CuO}_2$  planes by replacing spin-1/2 copper ions by nonmagnetic zinc or lithium. A large body of nuclear magnetic resonance (NMR) experiments on metallic and superconducting  $\text{YBa}_2\text{Cu}_3\text{O}_{6+x}$  ( $\text{YBCO}_{6+x}$ ) has demonstrated that such impurities generate a Curie term in the uniform susceptibility and a staggered spin-polarization cloud on neighboring Cu sites, in close analogy to the 1D systems discussed above [1]. NMR experiments on other families of cuprates are much more limited, because intrinsic disorder due to dopant atoms broadens the NMR lines, so that the effect of Zn impurities is masked by native disorder [10]. Inelastic-neutron-scattering (INS) experiments on both  $\text{YBCO}_{6+x}$  and  $\text{La}_{2-x}\text{Sr}_x\text{CuO}_4$  (LSCO) have revealed Zn-induced low-energy spin excitations, in qualitative agreement with the NMR results. In contrast to the 1D systems [4], however, a universal picture of the impurity-induced magnetism has not yet emerged in the 2D cuprates, because the spatial character of the impurity-induced low-energy spin dynamics in both materials appeared to be rather different: commensurate antiferromagnetic in  $\text{YBCO}_{6+x}$  [11,12] and incommensurate (IC) in LSCO [13]. Moreover, Zn-induced static incommensurate magnetism, which was observed in LSCO [13,14] and interpreted as evidence of pinning of fluctuating stripes [15], has thus far not been detected in  $\text{YBCO}_{6+x}$ . For this reason, and because LSCO exhibits static IC magnetic order at some doping levels even in the absence of spinless impurities [16], the universality of this order-from-disorder phenomenon has been questionable. These considerations have motivated us to revisit the effect of spinless impurities on the magnetic correlations of  $\text{YBCO}_{6.6}$ , a material with minimal native disorder that is well known for its large normal-state spin pseudogap [1].

The experiments were performed on an array of detwinned, coaligned  $\text{YBa}_2(\text{Cu}_{0.98}\text{Zn}_{0.02})_3\text{O}_{6.6}$  (henceforth  $\text{YBCO}_{6.6}:\text{Zn}$ ) single crystals of total mass 650 mg and superconducting  $T_c = 30$  K. A twin domain population ratio of 4:1 enabled us to discriminate spin excitations propagating along the  $a$  and  $b$  axes in the  $\text{CuO}_2$  planes, which is important in view of the recent observation of uniaxial, incommensurate magnetism in  $\text{YBCO}_{6.45}$  [17,18]. The INS measurements were carried out on the spectrometers IN8 (Institut Laue-Langevin, Grenoble), 4F2, 1T, 2T (Orphée, Laboratoire Léon Brillouin, Saclay), and PUMA (FRM-II, Garching), using either a pyrolytic-graphite (PG) (002) or a Si (111) monochromator in combination with a PG (002) analyzer. PG filters extinguished higher-order contaminations of the beam. The final wave vector was fixed to  $4.1 \text{ \AA}^{-1}$  for excitation energies  $E \geq 25$  meV, and to  $2.662 \text{ \AA}^{-1}$  or  $1.97 \text{ \AA}^{-1}$  for  $E < 25$  meV. Reference measurements were performed on a Zn-free  $\text{YBCO}_{6.6}$  array with  $T_c = 61$  K described previously [19]. Data on both arrays were compared by calibration measurements on the optical phonon at 42.5 meV following previous work [20], and by performing measurements under identical conditions. The wave vector transfers  $\mathbf{Q} = (H, K, L)$  are given in units of the reciprocal-lattice vectors  $\mathbf{a}^*$ ,  $\mathbf{b}^*$ , and  $\mathbf{c}^*$ .  $Q = (H, K)$  stands for 2D projections of  $\mathbf{Q}$ , and  $Q_{\text{AFM}} = (0.5, 0.5)$  is the wave vector characterizing antiferromagnetism in undoped  $\text{YBCO}_{6.0}$ .

Figures 1(a) and 1(b) show INS scans taken along the  $a$  axis of  $\text{YBCO}_{6.6}:\text{Zn}$  at  $E = 5$  meV, well below the spin pseudogap of pristine  $\text{YBCO}_{6.6}$ . A pair of well separated IC peaks symmetrically displaced from  $Q_{\text{AFM}}$  is observed consistently in two Brillouin zones on top of an extraneous background arising from the sample mount. The background is independent of the sample orientation and can be readily subtracted [Fig. 1(c)]. The signal is absent at  $L = 0$  and vanishingly small at large  $|\mathbf{Q}|$ , and can thus be ascribed to acoustic spin fluctuations [20]. Very similar peaks are also observed at  $E = 7$  and 10 meV [Figs. 1(d) and 1(e)]. As scans along the  $b$  axis are peaked at  $Q_{\text{AFM}}$ , the excitations are characteristic of uniaxial IC magnetism. Since low-energy spin excitations of comparable intensity are not observed in control experiments on pristine  $\text{YBCO}_{6.6}$  (see below), they can be identified as a result of Zn substitution.

The incommensurability of the impurity-induced spin excitations eluded detection in previous INS experiments on  $\text{YBCO}_{6+x}:\text{Zn}$  [11,12] for three reasons: First, the signal from the previously investigated twinned crystals consists of equal contributions from two twin domains, so that the IC character is less apparent. Second, earlier studies were performed in the scattering plane spanned by the vectors  $\mathbf{Q} = (1, 1, 0)$  and  $(0, 0, 1)$ , which does not include the IC wave vector. Third, the effective momentum-space resolution in the latter configuration is poorer than in the present experiment, because the long, vertical axis of the resolution ellipsoid is parallel to the  $\text{CuO}_2$  planes.

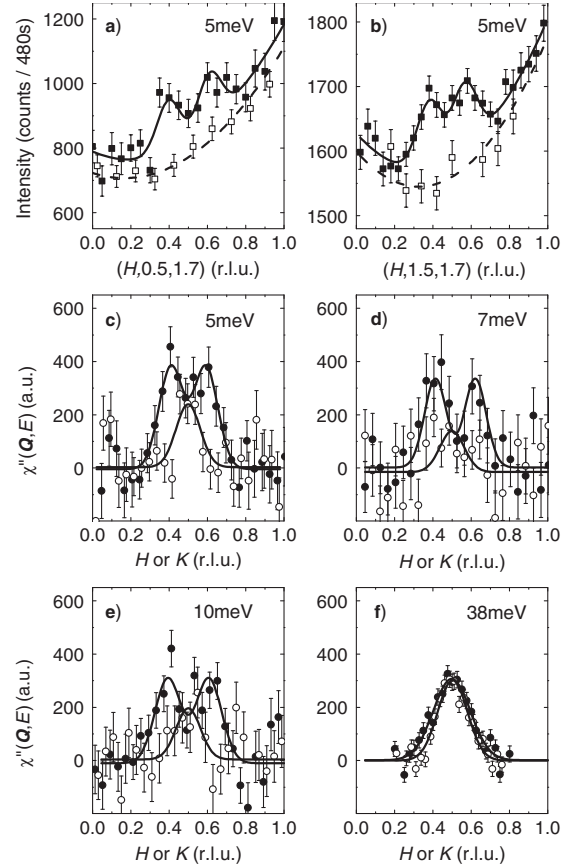


FIG. 1. Constant-energy scans in  $\text{YBCO}_{6.6}:\text{Zn}$  at  $T = 10$  K. (a, b) Uncorrected scans along (a)  $\mathbf{Q} = (H, 0.5, 1.7)$  and (b)  $(H, 1.5, 1.7)$ . The extraneous background was determined by rotating the sample by (a)  $30^\circ$ , (b)  $10^\circ$  and repeating the scans (open symbols). (c–f) Background-corrected scans along  $\mathbf{Q} = (H, 1.5, 1.7)$  (solid symbols) and  $(1.5, K, 1.7)$  (open symbols) at  $E = 5, 7, 10$ , and 38 meV.

The INS profiles were fitted to Gaussians centered at  $Q_{\text{AFM}} \pm (\delta, 0)$  [lines in Figs. 1(c)–1(e)]. In the range  $E = 5$ –10 meV, both the incommensurability  $\delta = 0.10 \pm 0.05$  and the intrinsic half-width-at-half-maximum  $\Delta Q = 0.055 \pm 0.025$  extracted from these fits were found to be energy independent within the error. The incommensurability is consistent with the one that characterizes excitations above the spin pseudogap of pristine  $\text{YBCO}_{6.6}$  [19], but significantly larger than the one observed in  $\text{YBCO}_{6.45}$  [17]. This confirms that the Zn content and the doping level are independent control parameters [1]. Models according to which Zn impurities reduce the hole doping level [21,22] are inconsistent with our data. The intrinsic momentum width translates into a length scale of  $\xi = 2.9a$ , where  $a$  is the in-plane lattice spacing. This represents a lower bound on the intrinsic coherence length of the spin fluctuations, because inhomogeneous broadening (arising from the doping dependence of  $\delta$  in combination with a possible slight nonuniformity of the doping level) may also contribute to  $\Delta Q$ . The value of  $\xi$  determined in this way is in good agreement with NMR data [23,24] and comparable to  $5.8a$ ,

the mean distance between Zn impurities in the  $\text{CuO}_2$  planes.

In view of the sharp excitation peaks, we have investigated the presence of magnetic order in  $\text{YBCO}_{6.6}:\text{Zn}$ . Since a quasielastic neutron signal like the one observed in  $\text{YBCO}_{6+x}$  for  $x \leq 0.45$  (Refs. [18,25]) could not be detected above background, we performed muon-spin-relaxation ( $\mu\text{SR}$ ) measurements, which are well suited to search for weak magnetic order. The experiments were performed with the GPS setup at the  $\pi M3$  beam line at the Swiss muon source  $S\mu S$  at the Paul Scherrer Institute, Villigen, Switzerland. The  $\mu\text{SR}$  spectra of  $\text{YBCO}_{6.6}:\text{Zn}$  as well as reference spectra of Zn-free  $\text{YBCO}_{6.6}$  and  $\text{YBCO}_{6.45}$  [Fig. 2(a)] were fitted to the relaxation function  $P(t) = P(0) \exp[-(\lambda t)^\beta] \times f_{\text{KT}}(t)$  that consists of the product of a stretched exponential and a Kubo-Toyabe function ( $f_{\text{KT}}$ ), which account for the contribution of the electronic and nuclear magnetic moments, respectively. For  $\text{YBCO}_{6.6}$  the relaxation is dominated by nuclear moments, suggesting the absence of static or slowly fluctuating electronic moments.

The  $\text{YBCO}_{6.6}:\text{Zn}$  spectra exhibit a more rapid depolarization at temperatures below  $\sim 10$  K [Fig. 2(a)], which is a signature of dominant contributions from electronic moments. The absence of a precession frequency indicates that these electronic moments are either static and disordered or slowly fluctuating. Additional longitudinal-field measurements were performed in order to discriminate between these scenarios [Fig. 2(b)]. The spectra were fitted with an Abragam relaxation function as described in Ref. [26] for polycrystalline samples. (A constant offset was added to account for the larger nonrelaxing signal of our single crystals.) The amplitude of the relaxing signal is already significantly reduced by a small longitudinal field of 25 Oe and almost vanishes at 250 Oe [Fig. 2(b)]. This is the hallmark of static and disordered magnetic moments [27]. The obtained values of  $\beta \sim 0.4$  for  $\text{YBCO}_{6.45}$  and  $\beta \sim 0.7$  for  $\text{YBCO}_{6.6}:\text{Zn}$  are characteristic of a spatially nonuniform distribution of the magnetic moment ampli-

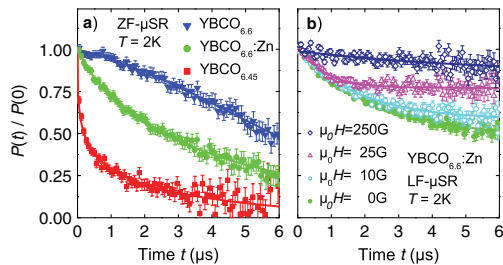


FIG. 2 (color online). (a) Zero-field and (b) longitudinal-field  $\mu\text{SR}$  data for  $\text{YBCO}_{6.6}:\text{Zn}$  at  $T = 2$  K. Panel (a) also shows data on  $\text{YBCO}_{6.6}$  and  $\text{YBCO}_{6.45}$ . The different amplitudes of the nonrelaxing signals in the ZF spectra of  $\text{YBCO}_{6.6}:\text{Zn}$  in panels (a) and (b) arise because these were measured in different geometries where the muon spin was rotated by  $\sim 60^\circ$  and  $0^\circ$ , respectively, with respect to the muon beam direction. The lines are the results of fits described in the text.

tude [14]. These observations confirm prior  $\mu\text{SR}$  results [1,28,29] according to which spinless impurities extend the range of magnetic order in the phase diagram of  $\text{YBCO}_{6+x}$  up to  $x \sim 0.7$ . The low-energy INS data (Fig. 1) and the close similarity between the  $\mu\text{SR}$  spectra of  $\text{YBCO}_{6.6}:\text{Zn}$  and those of pure  $\text{YBCO}_{6.45}$  [Fig. 2(a)] now indicate that this order is incommensurate, in contrast to the commensurate antiferromagnetism suspected on the basis of prior INS data on  $\text{YBCO}_{6+x}:\text{Zn}$  [11,12].

We now describe the behavior of the spin system at higher temperatures and excitation energies. At  $T = 70$  K (that is, above  $T_c$  of both  $\text{YBCO}_{6.6}$  and  $\text{YBCO}_{6.6}:\text{Zn}$ ), low-energy IC fluctuations persist in  $\text{YBCO}_{6.6}:\text{Zn}$  without significant thermal broadening [Fig. 3(a)], and remain much more intense than those in  $\text{YBCO}_{6.6}$  [Fig. 3(b)]. The onset temperature of the IC intensity in  $\text{YBCO}_{6.6}:\text{Zn}$  is  $\sim 150$  K [Fig. 3(c)], comparable to the onset of the spin pseudogap in  $\text{YBCO}_{6.6}$  documented by NMR [1]. This shows that Zn substitution restores low-energy spin fluctuations not only in the superconducting state, but also in the pseudogap state. The characteristic temperature for the Zn-induced enhancement of the spin dynamics is also comparable to the onset temperature of IC spin fluctuations in  $\text{YBCO}_{6.45}$ , which provides evidence for an electronic nematic state [17].

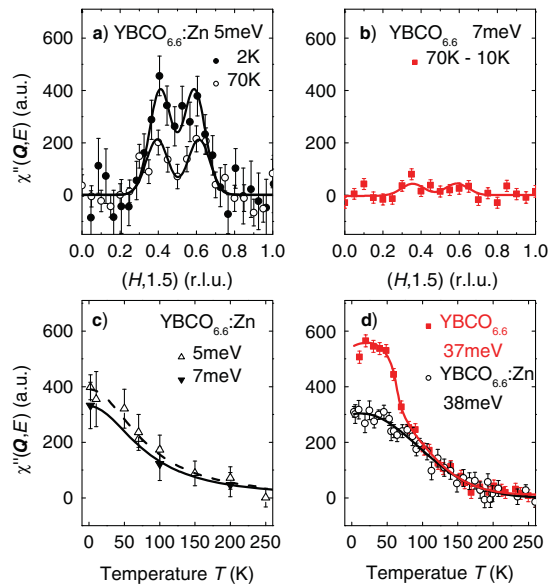


FIG. 3 (color online). Temperature dependence of the spin fluctuation intensity. (a, b) Scans of the dynamical magnetic susceptibility,  $\chi''(\mathbf{Q}, E)$  (derived from the INS data by correcting for the detailed-balance factor), around  $\mathbf{Q} = (0.5, 0.5, 1.7)$  in Zn-substituted and Zn-free  $\text{YBCO}_{6.6}$  at energies and temperatures marked in the legend. The data were background-corrected as described in Fig. 1. The lines are the results of fits described in the text. (c) Amplitude of  $\chi''$  in  $\text{YBCO}_{6.6}:\text{Zn}$  at  $E = 5$  and 7 meV extracted from fits to constant-energy scans. (d) Amplitude of  $\chi''$  for  $\text{YBCO}_{6.6}:\text{Zn}$  ( $\text{YBCO}_{6.6}$ ) at  $E = 38$  (37) meV. The lines are guides to the eye.



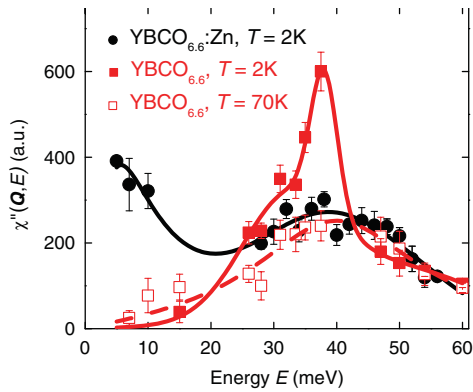


FIG. 4 (color online). Energy dependence of the peak susceptibility  $\chi''$  at  $T = 2$  K extracted from constant-energy scans on  $\text{YBCO}_{6.6}:\text{Zn}$  and  $\text{YBCO}_{6.6}$ . Normal-state data on pure  $\text{YBCO}_{6.6}$  are shown for comparison. The lines are guides to the eye.

A converse spectral-weight shift is observed at higher energies. Pure  $\text{YBCO}_{6.6}$  exhibits a sharp resonant mode with energy  $E_{\text{res}} = 38$  meV in the superconducting state [19,20], which is manifested by a sharp enhancement of the spin fluctuation intensity for  $E \sim E_{\text{res}}$  below  $T_c$  [Fig. 3(d)]. While  $\text{YBCO}_{6.6}:\text{Zn}$  exhibits a similar narrowing of the magnetic response around  $Q_{\text{AFM}}$  and  $E = 38$  meV as pure  $\text{YBCO}_{6.6}$  [Fig. 1(f)], followed by a dispersion away from  $Q_{\text{AFM}}$  at higher energies (not shown), the superconductivity-induced anomaly is obliterated by Zn substitution [Fig. 3(d)]. This is consistent with previous INS studies close to optimal doping that had demonstrated progressive weakening of the resonant mode with increasing Zn content without significant renormalization of its characteristic energy [30,31].

Figure 4 provides a synopsis of the spin excitation spectra of  $\text{YBCO}_{6.6}$  and  $\text{YBCO}_{6.6}:\text{Zn}$ . The  $\text{YBCO}_{6.6}:\text{Zn}$  spectrum at low temperatures is closely similar to the normal-state spectrum of  $\text{YBCO}_{6.6}$ , except for the strongly enhanced intensity at low energies that goes along with the appearance of IC magnetic order. The low-temperature spectrum of  $\text{YBCO}_{6.6}$ , on the other hand, is dominated by the sharp magnetic resonant mode at 38 meV, which is a signature of the superconducting state [20]. Fingerprints of both forms of collective electronic order are thus clearly apparent in the spin excitation spectrum, and the spectral-weight redistribution induced by Zn substitution demonstrates that spinless impurities nucleate static IC magnetism at the expense of superconductivity. This conclusion is consistent with the behavior expected in the vicinity of a quantum critical point separating both phases, and with prior  $\mu\text{SR}$  studies that had indicated a local suppression of the superfluid density around Zn impurities [32,33]. The two-phase competition also explains the extreme sensitivity of the magnetic resonant mode to a minute concentration of Zn impurities [30,31], which is difficult to explain in the framework of the random-phase approximation commonly used to describe the origin of this mode [34].

In conjunction with prior data on LSCO [13], our experiments indicate a universal order-from-disorder phenomenology for copper oxides with 2D electronic structure, closely analogous to the one previously established for quasi-1D quantum magnets [2–4]. In contrast to the latter systems, however, the spin excitations in the layered copper oxides are incommensurate. Our demonstration that the incommensurability in the  $\text{YBCO}_{6+x}$  system is independent of impurity concentration and controlled by the density of itinerant charge carriers, as previously shown for LSCO [13,16], explains the difference to the Mott-insulating 1D systems and further underscores the universality of impurity-induced spin correlations in low-dimensional quantum magnets.

We acknowledge discussions with E. Fradkin, P.J. Hirschfeld, H. Y. Kee, S. A. Kivelson, and O.P. Sushkov, and financial support by the DFG under Grant No. FOR538.

\*b.keimer@fkf.mpg.de

†yvan.sidis@cea.fr

- [1] For a review, see H. Alloul *et al.*, *Rev. Mod. Phys.* **81**, 45 (2009).
- [2] M. Hase *et al.*, *Phys. Rev. Lett.* **71**, 4059 (1993).
- [3] M. Azuma *et al.*, *Phys. Rev. B* **55**, R8658 (1997).
- [4] J. Bobroff *et al.*, *Phys. Rev. Lett.* **103**, 047201 (2009).
- [5] S. Sachdev *et al.*, *Science* **286**, 2479 (1999).
- [6] M. A. Metlitski and S. Sachdev, *Phys. Rev. B* **76**, 064423 (2007).
- [7] R. L. Doretto and M. Vojta, *Phys. Rev. B* **80**, 024411 (2009).
- [8] S. Wessel *et al.*, *Phys. Rev. Lett.* **86**, 1086 (2001).
- [9] M. Schmid *et al.*, *New J. Phys.* **12**, 053043 (2010).
- [10] J. Bobroff *et al.*, *Phys. Rev. Lett.* **89**, 157002 (2002).
- [11] Y. Sidis *et al.*, *Phys. Rev. B* **53**, 6811 (1996).
- [12] K. Kakurai *et al.*, *Phys. Rev. B* **48**, 3485 (1993).
- [13] H. Kimura *et al.*, *Phys. Rev. Lett.* **91**, 067002 (2003).
- [14] C. Panagopoulos *et al.*, *Phys. Rev. B* **69**, 144510 (2004).
- [15] S. A. Kivelson *et al.*, *Rev. Mod. Phys.* **75**, 1201 (2003).
- [16] M. Kofu *et al.*, *Phys. Rev. Lett.* **102**, 047001 (2009).
- [17] V. Hinkov *et al.*, *Science* **319**, 597 (2008).
- [18] D. Haug *et al.*, *Phys. Rev. Lett.* **103**, 017001 (2009).
- [19] V. Hinkov *et al.*, *Nature Phys.* **3**, 780 (2007).
- [20] H. F. Fong *et al.*, *Phys. Rev. B* **61**, 14773 (2000).
- [21] I. G. Kaplan, J. Soullard, and J. Hernandez-Cobos, *Phys. Rev. B* **65**, 214509 (2002).
- [22] A. A. Abrikosov, *Physica (Amsterdam)* **397C**, 77 (2003).
- [23] M.-H. Julien *et al.*, *Phys. Rev. Lett.* **84**, 3422 (2000).
- [24] S. Ouazi *et al.*, *Phys. Rev. B* **70**, 104515 (2004).
- [25] C. Stock *et al.*, *Phys. Rev. B* **73**, 100504(R) (2006).
- [26] A. Keren, *Phys. Rev. B* **50**, 10039 (1994).
- [27] Y. J. Uemura *et al.*, *Phys. Rev. B* **31**, 546 (1985).
- [28] P. Mendels *et al.*, *Phys. Rev. B* **49**, 10035 (1994).
- [29] C. Bernhard *et al.*, *Phys. Rev. B* **58**, R8937 (1998).
- [30] H. F. Fong *et al.*, *Phys. Rev. Lett.* **82**, 1939 (1999).
- [31] Y. Sidis *et al.*, *Phys. Rev. Lett.* **84**, 5900 (2000).
- [32] C. Bernhard *et al.*, *Phys. Rev. Lett.* **77**, 2304 (1996).
- [33] B. Nachumi *et al.*, *Phys. Rev. Lett.* **77**, 5421 (1996).
- [34] N. Bulut, *Phys. Rev. B* **61**, 9051 (2000).